

$$k_\alpha \bar{I}(\mathbf{k}, t) \equiv \int (c^2 - \frac{3}{2}) \bar{H}_\beta(\mathbf{c}, \mathbf{k}, t) d^3c$$

$$= ik_\alpha P(1 - e^{-t}) \{ e^{-t} - \frac{1}{4} k^2 (1 - e^{-t})^2 \}. \quad (\text{A7})$$

In the final expression for the density response we encountered

$$\bar{J}^s(\mathbf{k}, t) \equiv \int \bar{J}(\mathbf{c}, \mathbf{k}, t) d^3c = -\frac{1}{3} k^2 P(1 - e^{-t})^2. \quad (\text{A8})$$

We thus have

$$\bar{S} = \sum_{n=0}^4 S_n; \quad S_0 = -\frac{1}{6} ik^2, \quad S_1 = \frac{2}{3} i(1 + \frac{3}{4} k^2),$$

$$S_2 = -\frac{2}{3} i(1 + \frac{3}{4} k^2), \quad S_3 = \frac{1}{6} ik^2, \quad S_4 = 0; \quad (\text{A9})$$

$$K = \sum_{n=0}^4 k_n D_n, \quad k_0 = \frac{1}{2} k^4, \quad k_1 = \frac{4}{3} (-\frac{1}{2} k^2 - \frac{1}{4} k^4),$$

$$k_2 = \frac{4}{3} (k^2 + \frac{3}{8} k^4 + \frac{3}{2}),$$

$$k_3 = -\frac{2}{3} (k^2 + \frac{1}{2} k^4), \quad k_4 = \frac{1}{2} k^4; \quad (\text{A10})$$

$$\bar{I} = \sum_{n=0}^4 i_n D_n, \quad i_0 = -\frac{1}{4} k^2 i, \quad i_1 = i(1 + \frac{3}{4} k^2),$$

$$i_2 = -i(1 + \frac{3}{4} k^2), \quad i_3 = -\frac{1}{4} ik^2, \quad i_4 = 0; \quad (\text{A11})$$

$$\bar{J}^s = \sum_{n=0}^4 j_n D_n, \quad j_0 = -\frac{1}{3} k^2, \quad j_1 = \frac{2}{3} k^2,$$

$$j_2 = -\frac{1}{3} k^2, \quad j_3 = j_4 = 0. \quad (\text{A12})$$

Heat Currents in Liquid Helium II: Temperature and Velocity Fields in Large Channels*

M. V. RICCI AND M. VICENTINI-MISSONI

Istituto di Fisica, Università di Roma, Rome, Italy

(Received 11 January 1967)

A detailed study of the distribution of normal fluid velocity and temperature in a large channel has been made. For very low heat input, the normal fluid velocity is constant along the flow direction, in agreement with the linear theory of the two-fluid model. However, for large heat input values, anomalous distributions with large gradients confined to restricted space regions are observed both for the velocity and the temperature. The transition between the two flow regimes is seen to correspond to a critical superfluid velocity which is temperature-independent in the range 0.88–1.92°K. The supercritical flow is then interpreted as due to the presence of vorticity in the superfluid.

INTRODUCTION

IN helium II a temperature difference between the ends of a channel gives rise to a convection current of normal fluid and superfluid.¹ The analytical relationship between the temperature gradient and the normal fluid velocity \mathbf{v}_n may be sought by solving the hydrodynamical equations of the two-fluid model:

$$\rho_s \frac{d\mathbf{v}_s}{dt} = -\frac{\rho_s}{\rho} \nabla p + \rho_s S \nabla T, \quad (1)$$

$$\rho_n \frac{d\mathbf{v}_n}{dt} = -\frac{\rho_s}{\rho} \nabla p - \rho_s S \nabla T + \eta_n \nabla^2 \mathbf{v}_n, \quad (2)$$

$$\frac{\partial \rho}{\partial t} + \text{div}(\rho_s \mathbf{v}_s + \rho_n \mathbf{v}_n) = 0, \quad (3)$$

$$\frac{\partial \rho S}{\partial t} + \text{div}(\rho S \mathbf{v}_n) = \dot{\sigma}_n. \quad (4)$$

In a counterflow experiment there is no net mass transport ($\rho_s \mathbf{v}_s + \rho_n \mathbf{v}_n = 0$), and in stationary motion the continuity equation is then identically satisfied. In the limit of low velocities, where the entropy dissipation of the normal fluid may be considered negligible, it follows for a stationary unidirectional flow from the entropy conservation Eq. (4) that the normal fluid velocity is independent of the flow coordinate (say z direction). Then in a linear approximation the solution of the hydrodynamical equations gives a direct proportionality between temperature gradient and normal fluid velocity (or heat current density \dot{q} defined by $\dot{q} = \rho S T v_n$):

$$\frac{dT}{dz} = c \frac{\eta_n}{\rho S} \langle v_n \rangle \quad (5)$$

where $\langle v_n \rangle$ is the value of v_n averaged across the section of the channel and c a geometrical constant.

If the nonlinear terms cannot be neglected, then for a stationary flow in one direction, \mathbf{v}_n and \mathbf{v}_s may be functions of all coordinates and the analytical solution

* Work supported by Consiglio Nazionale delle Ricerche, Rome, Italy.

¹ See, for instance, K. R. Atkins, *Liquid Helium* (Cambridge

University Press, New York, 1959); or F. London *Superfluids* (John Wiley & Sons, Inc., New York, 1954), Vol. II.

of the equations is nearly impossible. Moreover, it is a matter of controversy whether the equations given above completely describe the flow at large velocities, in which case the critical velocity should be due to a hydrodynamical instability like that arising in the transition to turbulence in a classical fluid. On the other hand, if the critical velocity is due to the creation of quantized vorticity,^{2,3} other nonlinear terms should be added to the equations in order to account for the interaction between vortices and normal fluid.^{4,5} An example of such terms is given by the Gorter-Mellink-Vinen mutual friction force

$$\mathbf{F}_{sn} = A\rho_s\rho_n[|\mathbf{v}_s - \mathbf{v}_n|^2 - v_0^2](\mathbf{v}_s - \mathbf{v}_n), \quad (6)$$

which was introduced to explain some experiments concerning the dependence on the heat input \dot{q} of the temperature difference between the ends of a channel. The introduction of a mutual-friction-force term like (6) gives a satisfactory account of a number of counterflow experiments, but not of experiments involving other types of motion.⁶

In a previous paper,⁷ hereafter referred to as I, there were reported some experiments performed in our laboratory to measure the normal fluid velocity and the temperature in a counterflow of normal fluid and superfluid in channels of various geometries and dimensions. Such experiments gave evidence that for very low heat input values \dot{q} , the normal fluid velocity is, in agreement with the predictions of the linear theory of the two-fluid model, a constant along the flow direction and related to \dot{q} by $v_n = v_n^0 = \dot{q}/\rho ST$. However, for fairly large \dot{q} values ($\dot{q} \gtrsim 5 \text{ mW/cm}^2$), a large gradient in v_n along the coordinate in the flow direction is present. The velocity does not seem to vary linearly with z : But there are indications of a complex velocity distribution; in some positions the velocity may also be found larger than v_n^0 . In I the transition between the two flow regimes was not studied extensively. The experimental results at one value of the bath temperature were interpreted as due to instability with respect to vorticity in the superfluid. Because of the anomalous thermal conductivity in helium II, an indirect check of the existence of a gradient in the normal fluid velocity at large \dot{q} values (supercritical flow) was given by measurements of the temperature distribution along the flow direction in a channel. These measurements showed the nonuni-

formity of the temperature gradient in the direction.⁸ However, in these experiments velocity and temperature were not measured simultaneously in the same channel, and thus it was not possible to establish any empirical connection between the two parameters. Such a connection, as well as a better knowledge of the velocity distribution, may throw some light on the mechanism involved in the range of large velocities and on the critical phenomenon itself. Moreover, an extended study of the transition, by varying the bath temperature in the range $1.0^\circ\text{K}-\lambda$ point, may contribute to an understanding of the mechanism of the instability.

EXPERIMENTAL APPARATUS AND PROCEDURE

The aim of the present work is the simultaneous determination of velocity and temperature fields in the same channel. In order to check previous results, we have used an apparatus with geometrical characteristics similar to those of the channel A used in I: rectangular cross section $0.4 \times 0.8 \text{ cm}^2$, length 8.0 cm. In Fig. 1A a schematic view of the apparatus is shown. Because of the heat flow due to the heater H in a direction perpendicular to the electric field E , the ionic beam produced by the polonium source suffers a displacement which is registered as a change in the currents of electrodes 2 and 4. The normal fluid velocity $\langle v_n \rangle$ is related to such changes, say ΔI_i , by

$$\langle v_n \rangle_i = c\mu E \Delta I_i / I_3. \quad (7)$$

The subscript i on $\langle v_n \rangle$ indicates the electrode at which $\langle v_n \rangle$ is measured; the factor $c = (d_i/s)(I_3/I_i)_\infty$ accounts for geometrical corrections, as explained in I; μ is the ionic mobility; and I_3 is the current received by the central electrode 3.

With one polonium source the determination of the velocity in two positions is obtained. Then the amount of information on the velocity field depends on the number of sources which may be placed along the channel. The source length can be reduced to about 1.0 cm, thus allowing v_n measurements at a spacing not less than 0.5 cm. Taking into account the lengths of the measuring and guard electrodes, at most four ionic beams could be placed on the 8.0-cm length. However, considering the heat losses due to the larger number of wires necessary for each ionic beam detection, a two-source apparatus was preferred. More detailed information is then obtained by varying the positions of the two sources with respect to each other and to the heater (B and C of Fig. 1). The heaters used were a 1000Ω , $\frac{1}{8}W$ resistor "Metal lux" or a 1000Ω Constantan wire.

The velocity value as measured from the displacement of the ionic beam is a value averaged across one section

² R. P. Feynman, *Progress in Low Temperature Physics* (North-Holland Publishing Company, Amsterdam, 1955), Vol. I, p. 45.

³ V. P. Peshkov, *Progress in Low Temperature Physics* (North-Holland Publishing Company, Amsterdam, 1955), Vol. IV, p. 1.

⁴ C. J. Gorter and J. H. Mellink, *Physica* **15**, 285 (1949).

⁵ W. F. Vinen, *Proc. Roy. Soc. (London) Ser. A* **240**, 114 (1957); **242**, 493 (1957); **243**, 400 (1957).

⁶ T. M. Wiarda, B. van der Heyden, and H. C. Kramers, in *Proceedings of the Ninth Conference on Low Temperature Physics, Columbus, Ohio, 1964*, edited by J. G. Daunt, D. V. Edwards, and M. Yakub (Plenum Press, Inc., New York, 1965), p. 284.

⁷ M. Vicentini-Missoni and S. Cunsolo, *Phys. Rev.* **144**, 196 (1966).

⁸ The hypothesis of a nonuniform temperature gradient has been put forward independently to explain some results on the thermal conductivity of liquid helium II in narrow channels. [H. H. Madden, H. V. Bohm, M. D. Cowan, and E. C. Alcaraz, *Phys. Rev.* **139**, A1783 (1965)].

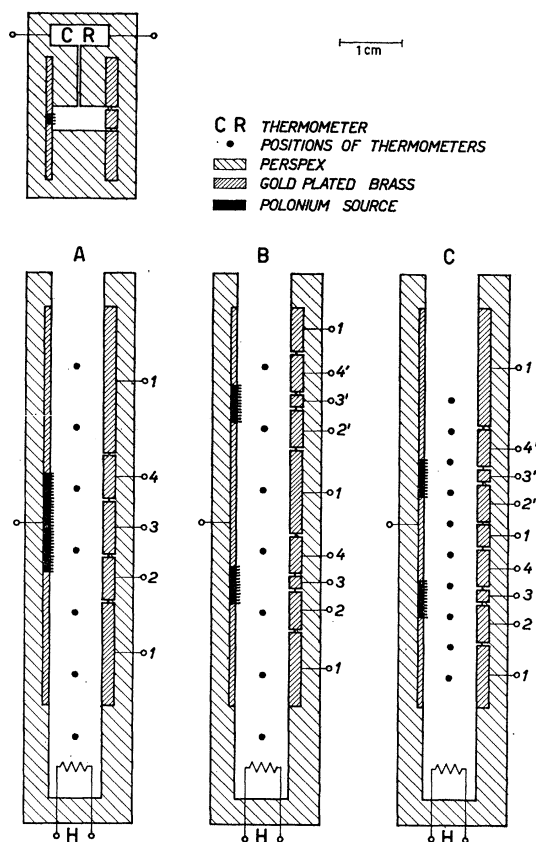


FIG. 1. Schematic view of the apparatus.

of the channel. Then in order to correlate the temperature with the velocity distribution, the temperature should also be averaged over the cross section. For a flow in one direction it follows from Eqs. (1) and (2) that the temperature is dependent only on z , not on the coordinates in the section of the channel. If the flow is not purely one-directional, the dependence of T on these coordinates cannot be excluded. However, if no change in the flow regime is present along the length of the channel, the temperature profile in the cross section should be independent of z . Then, as we are interested in the dependence of T on z only, it is preferable to select the location of the temperature probes so as to introduce a minimum perturbation in the flow. That is the case on the walls of the channel.

The thermometers, Allen Bradley $10 \Omega \pm 0.5\%$ $\frac{1}{2}W$ size carbon resistors, were held in one of the walls of the channel and communicated with it through small holes 0.05 cm in diam. The temperature difference between each thermometer and a reference thermometer in the bath is measured differentially. A decade resistor could be placed in series with either of the internal thermometers to equalize the measured resistances at a given temperature so that temperature differences could be measured directly. The sensitivity of the measurements was of the order of 10^{-5}°K .

The experimental procedure for each run was the following: On each electrode the current change, due to a heat input \dot{q} , was detected for at least two different values of the electric field E , with the only restriction that E should be less than the field corresponding to the critical velocity of the first discontinuity in the mobility.⁹ The values of \dot{q} ranged from as low as compatible with the sensitivity in the measurements (about 0.5 mW/cm^2) to the largest value for which the bath temperature could be controlled (about 70 mW/cm^2). We could thus detect the velocity distribution in the linear regime of flow, as well as in the supercritical regime and the threshold between the two regimes. Because of the large cross section of the channel, the accuracy of the temperature measurements was not enough to detect the subcritical distribution. Thus we will suppose that in this range there is, in agreement with the linear theory, a uniform temperature gradient in the z direction and try to establish a connection with the velocity distribution only for the supercritical range. Such a connection may be sought with the following procedure in the analysis of the experimental data: For each \dot{q} value for which $T(z)$ has been measured at a number of positions in the channel, one may calculate the value of (dT/dz) corresponding to the positions z_i where the velocity has been measured, and seek an empirical relation between $v_n(z_i)$ and $(dT/dz)_{z=z_i}$. However, for such a procedure to be applied, it is necessary that large changes in the temperature gradient be observed on a scale much larger than the distance between the thermometers. If this should not be the case, only a qualitative comparison between the two functions remains possible.

VELOCITY AND TEMPERATURE

A first series of runs was performed with apparatus A (Fig. 1). Typical results are shown in Fig. 2 for the velocity as a function of the heat input and in Fig. 3 for the temperature distribution in the channel at $T=0.95^\circ\text{K}$. There is a good check of previous results, as the points attributed to run C_3 were taken about three years ago with an apparatus of the same geometry and the same electrode positions. The velocity is not a constant along the flow direction; rather a change as large as 10% in a 1.5-cm distance is observed. Under the hypothesis of a uniform variation of v_n along z ($(d^2v_n/dz^2)=0$), the velocity gradient may be evaluated to be $\simeq 2 \text{ sec}^{-1}$. For a flow in one direction, we may compare the nonlinear terms $\rho_s v_s (dv_s/dz)$ and $\rho_n v_n (dv_n/dz)$ in the equations of motions with the thermal-force term $\rho_s S (dT/dz)$. From the temperature distribution of Fig. 3, we see that if the small-scale nonuniformities can be averaged over the distance between the thermometers, the order of magnitude of the thermal gradient at the positions of the electrodes will be $(dT/dz) \simeq 10^{-4}^\circ\text{K/cm}$. Therefore, with the measured values of velocity and

⁹ G. Careri, S. Cunsolo, and P. Mazzoldi, Phys. Rev. **136**, A303 (1964).

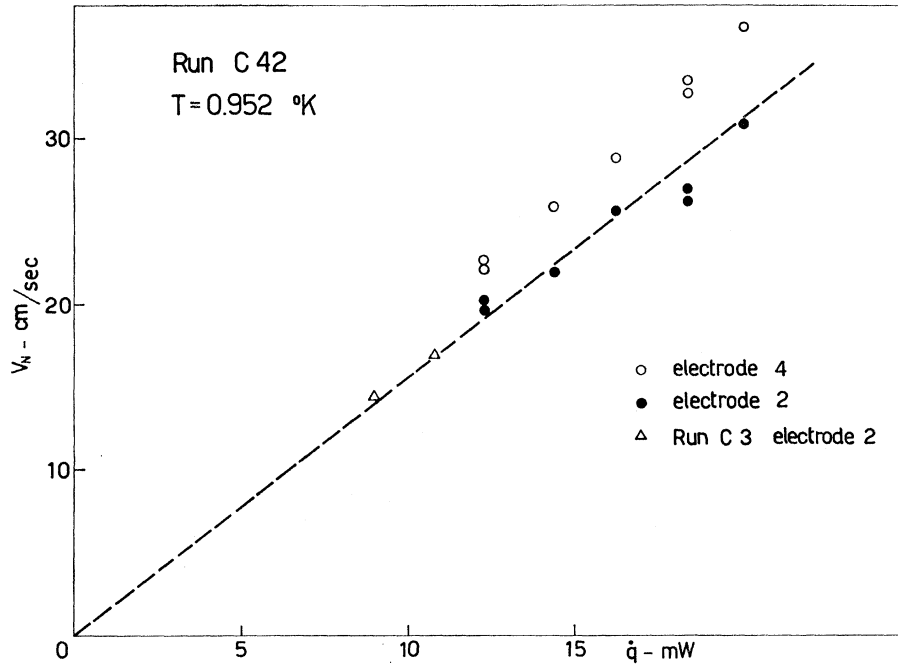


FIG. 2. Normal fluid velocity as a function of the heat input for channel A. The dashed line represents the relation $v_n = v_n^0 = \dot{q} / \rho S T$.

temperature gradients, the nonlinear terms are found to be still negligible, and, if the pressure gradient may still be considered to depend linearly on the velocity, one may hope to derive from the experimental dependence of (dT/dz) on v_n , empirical information on the mutual

friction force

$$F_{zn} = (dp/dz) - \rho S (dT/dz). \quad (8)$$

Because of the small-scale nonuniformities of the temperature distribution, the evaluation of the temperature gradient is not accurate. The values of (dT/dz) reported on a logarithmic plot as a function of the measured velocity seem to show a linear dependence with a slope of about 3 (see Fig. 4); that is,

$$(dT/dz) = \alpha(z, T) v_n^3. \quad (9)$$

This is exactly the kind of dependence which was de-

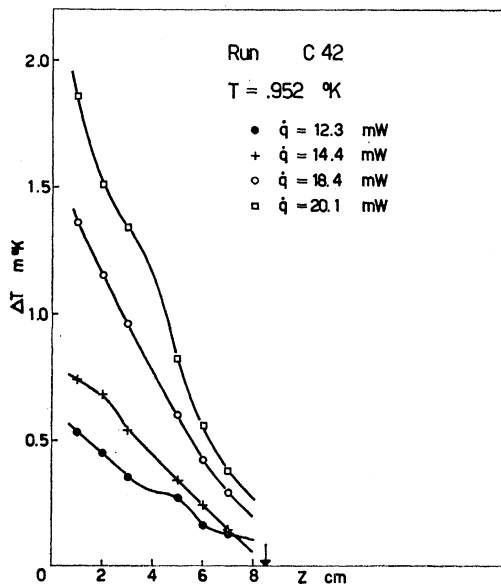


FIG. 3. Temperature distribution in channel A for different values of the heat input. Temperature differences are calculated with respect to the bath temperature. The lines are drawn simply to connect the experimental points and do not show any analytical relation. The arrow on the abscissa indicates the end of the channel.

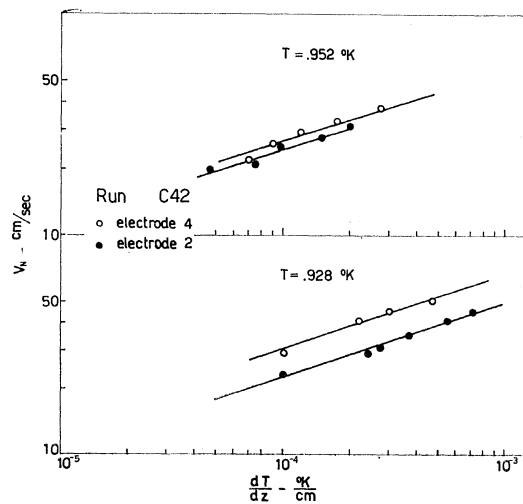


FIG. 4. Bilogarithmic plot of the normal fluid velocity versus temperature gradient calculated by Fig. 3.

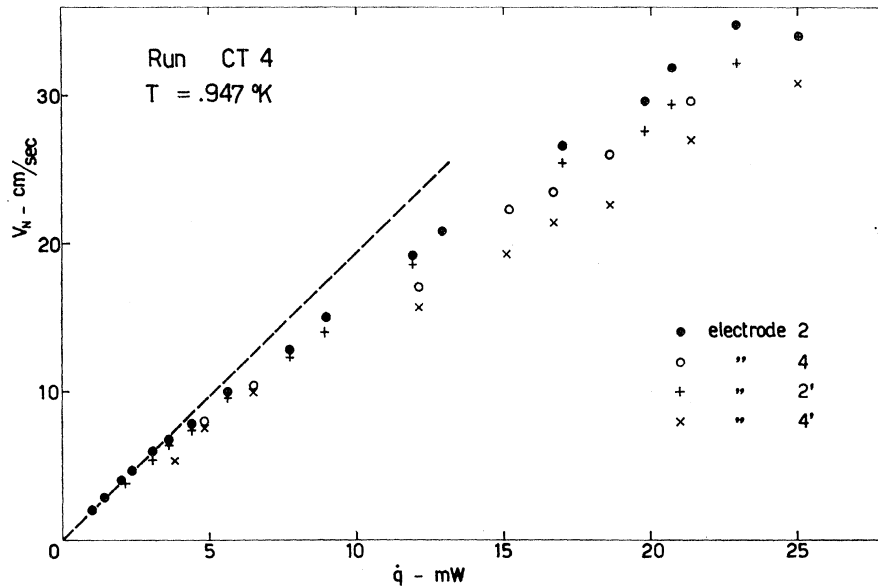


FIG. 5. Same as Fig. 2 for channel B.

rived from the experimental data on the temperature difference between the ends of a channel as a function of \dot{q} ^{10,11} under the hypothesis $v_n = \dot{q} / \rho S T = \text{constant}$, and $(dT/dz) = \text{constant} = (\Delta T/L)$.

However, the fact that the coefficient α in Eq. (9) is a function not only of T , but also of z , makes a big difference, and implies that the analytical relationship between (dT/dz) and v_n is more complex than (9) and must be sought through the complete solution of the hydrodynamical equations. Moreover, in the previous discussion we made some hypotheses concerning the behavior of the velocity and temperature gradients, such as the uniformity of the velocity gradient, which were based on very poor data on the velocity distribution. We must then seek more information on the distribution itself. This was done with apparatus B and C (Fig. 1) in which it was possible to measure the velocity at four positions simultaneously with the temperature distribution. While in apparatus B the thermometers were placed at a spacing of about 1 cm, just as in A, in apparatus C the spacing was 0.5 cm in order to see smaller scale details of the distribution.

A number of runs were performed with each apparatus in the temperature range 0.888–1.376°K and gave results which show that the behavior is qualitatively the same at all temperatures. An example is given by run CT4, which was obtained with apparatus B at a temperature $T = 0.947^\circ\text{K}$. Figure 5 shows the velocity as a function of \dot{q} for the four electrodes. At very low \dot{q} the agreement with the linear theory is evident.

From the plots of Fig. 5 the shape of the function $v_n(z)$ can be obtained, as illustrated in Fig. 6. The velocity gradient is not uniform: Since the function $v_n(z)$

has to be a continuous function of z and has to fit the experimental values, it must pass through a minimum and a maximum in the range $4 \leq z \leq 6$ cm. Since there is no theory available to explain this behavior, it would be better to have more experimental values of v_n as a function of z . This is also necessary if one wants to find a connection with the temperature distribution reported in Fig. 7.

This is done using the results obtained in different runs with the three different apparatus at about the same temperature. From the temperature distribution we check that the flow regime examined is the same. (See Fig. 8.) The slight disagreement between the temperature values measured in the different runs may be ascribed either to a slight difference in the bath temperature value or in the heater position, since in drawing such plots we took the cold end of the channel as a reference point. The velocity distribution is shown in the left part of Fig. 9. The agreement in the results obtained with

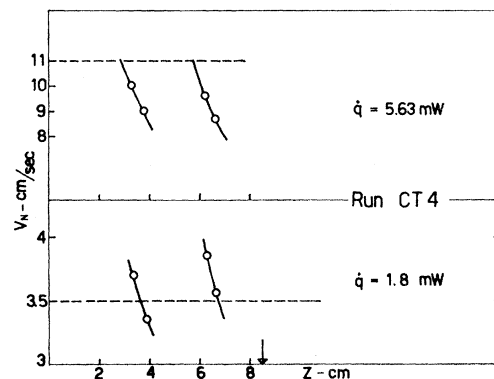


FIG. 6. Normal fluid velocity detected by the four electrodes of apparatus B. The dashed lines are calculated by $v_n = v_n^0 = \dot{q} / \rho S T$.

¹⁰ C. E. Chase, Phys. Rev. **127**, 361 (1962).

¹¹ E. F. Hammel and W. E. Keller, Phys. Rev. **124**, 1641 (1961).

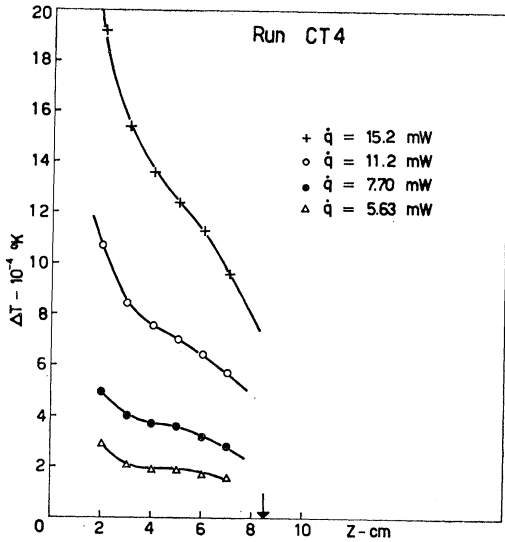


FIG. 7. Same as Fig. 3 for channel B.

the various apparatus at about the same position assures, together with the agreement in the temperature distribution, that one flow regime is being examined.

It may be seen that, in effect, in the region $4 \leq z \leq 7$ cm, $v_n(z)$ should pass through a minimum value and a maximum value. From the position of the experimental points, one concludes that the maximum is very pronounced, while the information about the minimum is scarce. An example of the velocity field at an appreciably higher value of the bath temperature is given in the right-hand side of Fig. 9 for $T = 1.376^\circ\text{K}$.

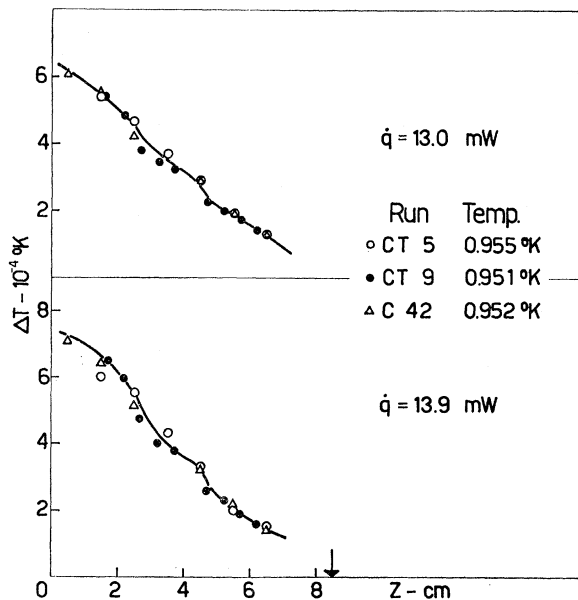


FIG. 8. Comparison of the temperature distributions for the three channels at about the same temperature and for the same value of the heat input.

Concerning the link between temperature and velocity, the temperature measurements with a spacing of 0.5 cm between the thermometers show that the scale of the changes in the thermal gradient is comparable to, or smaller than, the spacing itself. Therefore it is not possible to derive any quantitative expression for (dT/dz) as a function of v_n , and only a qualitative comparison between the shapes of the two distributions will be made. The fact that much larger changes in the velocity rather than in the temperature are detected may be understood by observing that if, as in the linear flow, the velocity is directly related to the temperature gradient, a large change in the velocity will correspond to a large change in the slope of the temperature distribution but not in the temperature itself. A maximum or minimum in the velocity corresponds to an inflection

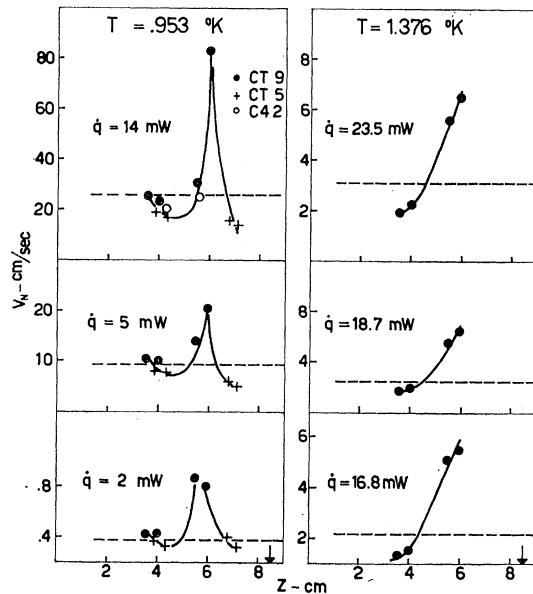


FIG. 9. Normal fluid velocity distributions obtained using the three apparatus of Fig. 1. Dashed lines calculated by $v_n = v_n^0 = \dot{q}/\rho ST$. The arrow indicates the end of the channels.

point in the temperature distribution. A close examination of the last distribution shows that such inflection points may exist in correspondence with the observed maximum and minimum in the velocity. Therefore we will assume that the velocity and temperature measurements check with one another, and we will restrict the discussion to the velocity results.

We will summarize the conclusions one may derive from the experimental results in the temperature range explored:

- (a) The velocity distribution is uniform for very low values of the heat current density.
- (b) As soon as a critical velocity has been overcome, the distribution shows a complex behavior with unexpected large gradients confined in somewhat restricted

space regions, in which the velocity appears to have a maximum value that is larger than the value one derives from the heat current input $v_n^0 = \dot{q}/\rho ST$.

(c) The position of the maximum does not depend strongly either on the heat input or on the bath temperature; however, a slight dependence may not be ruled out.

(d) The amplitude of the space regions in which the maximum is observed (that is, the distance between the two z values for which $v_n = v_n^0$) does not depend strongly on the heat input value.

(e) The behavior of the velocity in the space region explored strongly suggests that analogous behavior might be found in the rest of the channel. For instance, another maximum should be observed in the region between the heater and $z = 3.5$ cm. However, the measurement of the velocity through the deflection of an ionic beam is not suitable for the detection of such small scale variations and another method is required. As an example, the study of the drag exercised by the normal fluid on solid-hydrogen particles¹² should be able to give a number of details of the flow pattern.

THE CRITICAL VELOCITY

The experimental results reported above enable one to distinguish between two flow regimes: The first one is a regime in which the normal fluid velocity is constant in the flow direction and has a value which is in agreement with the definition of the heat current density made on the basis of the linear theory of the two-fluid model; the other one is a regime with a velocity field such that the value of (dv_n/dz) is a strong function of z itself. The transition between the two regimes is rather sharp and corresponds to an instability in an hydrodynamical sense, for which we may define a threshold as the lowest value of the heat current density \dot{q}_c for which the first regime is no longer stable. As is apparent from Fig. 9, such a threshold value is better determined at the z values for which the maximum in the velocity is observed, and is simply revealed by a variation of the slope in the experimental dependence of the change in the current measured at one of the electrodes on the heat current density (in the low-velocity regime of flow a linear dependence is observed). For the determination of the velocity distribution so far only positive ions were used since for these ions the mobility is known to be a constant whichever \dot{q} value produces the flow.¹³ However, the negative ions in the flow regime observed at low \dot{q} also give results in agreement with the linear theory,⁷ and therefore either positive or negative ions may be used to detect the threshold. As was discussed in I, it is not possible to rely on the results obtained with negative ions in the supercritical flow for the determina-

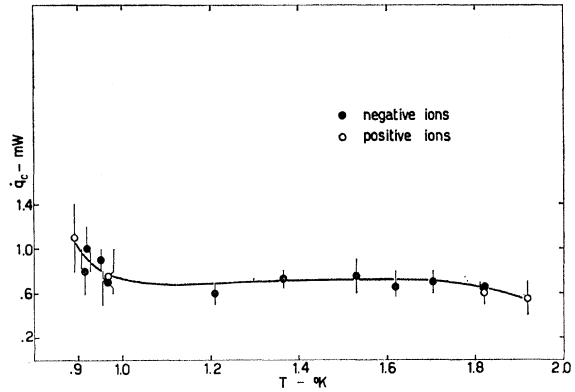


FIG. 10. Critical heat input versus temperature.

tion of the normal fluid velocity. The different behavior of the negative ions as a characteristic of the supercritical regime itself must be kept in mind.

Experimental determinations of the threshold have been done in the temperature range 0.88–1.92°K with positive and negative ions and at different z values, except at the higher temperatures, where, for sensitivity reasons, we looked only at the z values corresponding to the maximum. The results are given in Fig. 10. We point out the agreement between the results obtained with negative and positive ions and at the various positions along the channel. The results may be analyzed in terms of the various parameters characterizing the flow, namely, the superfluid velocity v_s , the normal fluid velocity v_n , the relative velocity $v_s - v_n$, a Reynolds number for the normal fluid

$$R_1 = \frac{\rho_n \langle v_n \rangle d}{\eta_n}$$

and the Reynolds numbers for the fluid as a whole

$$R_2 = \frac{\rho \langle v_n \rangle d}{\eta_n}, \quad R_3 = \frac{\rho (\langle v_n \rangle - \langle v_s \rangle) d}{\eta_n}$$

All these parameters have been calculated from the experimental \dot{q}_c values and are shown in Table I.

The behavior of the negative ions was observed not only through the beam deflection, but also through the detection of the total current produced by each source on the three facing electrodes. No appreciable change could be detected up to quite large \dot{q} values, where sharp decrease in the total current was detected, analogous to that observed in similar experiments,¹⁴ at a value \dot{q}' much larger than \dot{q}_c , and of the same order as found in those experiments. This threshold may be interpreted as connected with the trapping of negative ions by

¹² T. A. Kitchens, W. A. Steyert, R. D. Taylor, and P. P. Craig, Phys. Rev. Letters 14, 942 (1965).

¹³ G. Careri, S. Cunsolo, and M. Vicentini-Missoni, Phys. Rev. 136, A311 (1964).

¹⁴ G. Careri, F. Scaramuzzi, and J. O. Thomson, Nuovo Cimento 18, 957 (1960). See also G. Careri, F. Dupré, and P. Mazzoldi, in *Quantum Fluids*, edited by D. F. Brewer (North-Holland Publishing Company, Amsterdam, 1966), p. 305.

TABLE I. Critical parameters: q_c is the experimental critical heat input; v_{nc} and v_{sc} are the corresponding normal fluid velocity and superfluid velocity; d is the hydraulic diameter (0.53 cm)

$$R_{e1} = \frac{\rho_n v_{nc} d}{\eta_n}; \quad R_{e2} = \frac{\rho v_{sc} d}{\eta_n}; \quad R_{e3} = \frac{\rho (|v_{sc} - v_{nc}|) d}{\eta_n}.$$

Run	Ions	$T(^{\circ}\text{K})$	$q_c(\text{mW})$	$v_{nc}(\text{cm/sec})$	$v_{sc}(10^{-3} \text{ cm/sec})$	$ v_{sc} - v_{nc} (\text{cm/sec})$	R_{e1}	R_{e2}	R_{e3}	$v_{sc} d (10^{-3} \text{ cm}^2/\text{sec})$
CT6b	+	0.888	1.1 ± 0.3	3.16 ± 0.9	8.6 ± 2.3	3.15 ± 0.9	17 ± 4	6500 ± 1800	6500 ± 1800	4.5 ± 1.3
CT2	-	0.913	0.8 ± 0.2	2.0 ± 0.5	6.4 ± 1.5	2.0 ± 0.5	13.5 ± 3.5	4150 ± 1050	4150 ± 1050	3.6 ± 0.9
CT3	-	0.918	1.0 ± 0.2	2.3 ± 0.5	8.4 ± 1.6	2.3 ± 0.5	18.5 ± 3.5	5100 ± 1000	5100 ± 1000	4.4 ± 0.9
CT5	-	0.951	0.89 ± 0.09	1.6 ± 0.2	7.5 ± 0.7	1.6 ± 0.2	19 ± 2	3850 ± 450	3850 ± 450	4.0 ± 0.4
CT6a	-	0.967	0.7 ± 0.1	1.16 ± 0.16	6.4 ± 0.9	1.15 ± 0.16	16 ± 2	2840 ± 410	2840 ± 410	3.4 ± 0.5
CT6a	+	0.967	0.75 ± 0.25	1.24 ± 0.4	6.6 ± 2.0	1.23 ± 0.4	17 ± 5	3050 ± 1000	3050 ± 1000	3.5 ± 1.1
CT10	-	1.208	0.6 ± 0.1	0.20 ± 0.04	5.9 ± 1.0	0.19 ± 0.04	20 ± 4	700 ± 140	665 ± 140	3.1 ± 0.5
CT7	-	1.365	0.72 ± 0.07	0.10 ± 0.01	6.9 ± 0.7	0.09 ± 0.01	37 ± 3	480 ± 50	430 ± 50	3.7 ± 0.4
CT10	-	1.530	0.75 ± 0.15	$(47 \pm 10)10^{-3}$	7.5 ± 1.5	$(40 \pm 11)10^{-3}$	37 ± 8	300 ± 60	255 ± 100	4.0 ± 0.8
CT9	-	1.618	0.65 ± 0.15	$(28 \pm 6)10^{-3}$	6.1 ± 1.4	$(22 \pm 7)10^{-3}$	32 ± 8	175 ± 45	142 ± 45	3.2 ± 0.8
CT10	-	1.703	0.7 ± 0.1	$(22 \pm 3)10^{-3}$	7.4 ± 1.0	$(15 \pm 4)10^{-3}$	33 ± 5	142 ± 20	97 ± 26	3.9 ± 0.5
CT10	+	1.820	0.6 ± 0.1	$(12.5 \pm 2.1)10^{-3}$	7.1 ± 1.2	$(5.4 \pm 3.3)10^{-3}$	27.6 ± 3.2	80 ± 9	35 ± 21	3.75 ± 0.64
CT10	-	1.820	0.65 ± 0.05	$(13.6 \pm 1.0)10^{-3}$	7.7 ± 0.6	$(5.9 \pm 1.6)10^{-3}$	30 ± 2	87 ± 6	38 ± 11	4.1 ± 0.3
CT10	+	1.918	0.55 ± 0.15	$(8.4 \pm 2.3)10^{-3}$	7.5 ± 2.0	$(0.9 \pm 4.3)10^{-3}$	25 ± 7	54 ± 7	5.8 ± 28	4.0 ± 1.0

vortex lines. The shape of the velocity distribution does not change at the crossing of such threshold.

DISCUSSION

As pointed out above, the flow in a large channel shows a threshold phenomenon as a function of the velocity, corresponding to an instability between two flow regimes. The regime of flow established in the channel for low velocities is in agreement with the linear theory of the two-fluid model and therefore needs no more discussion. On the contrary, for an understanding of the flow regime established at high velocities, we must discuss at the same time the characteristic of this regime and its instability. We will begin with the instability. We have listed all the parameters which may be thought as characteristic of the threshold. Among them we have not listed a Gorter number as defined by Meservey,¹⁵

because the analytical expression for the mutual friction force as given by Gorter and Mellink⁴ is not in agreement with our results and no other expression for such a force is available.

The expected temperature dependence of the flow parameter governing the instability depends upon which parameter is considered relevant. If the instability is due to the creation of quantized vorticity, as proposed by Feynman and discussed by various authors, the characteristic parameter should be the superfluid velocity with respect to the boundaries or to the normal fluid, and the parameter itself will be temperature independent away from the λ point. If the instability corresponds to a transition to a turbulent flow in the normal fluid, the classical analogy tells us that the relevant parameter is a Reynolds number R_1 and the critical value should be $R_{e1} = 1300$, independent of temperature. The instability may also correspond to a transition to turbulence for the fluid as a whole, and in this case the parameter is a Reynolds number with the total density, that is, R_2 or R_3 . The critical value as predicted by the classical analogy is again 1300. However in this last case, the considerations of Tough¹⁶ can be applied, suggesting a dependence of the critical value on temperature: For higher temperature a lower R_e could be expected.

A close examination of Table I enables us to discard the hypothesis of a transition to turbulence in the normal fluid alone: The observed R_{e1} is too low, and temperature-dependent. Also, the possibility of ascribing the threshold we observed to a transition to turbulence of the fluid as a whole may be discarded, since either R_{e2} or R_{e3} is too large in the low-temperature limit. On the other hand, the superfluid velocity with

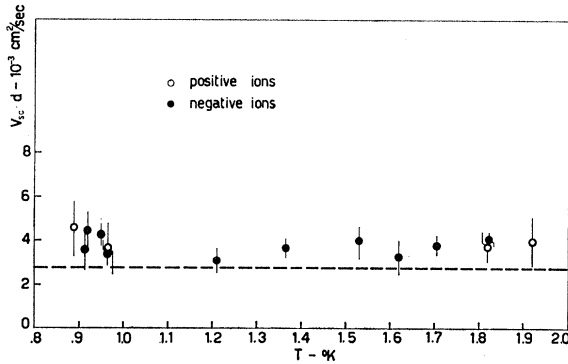


FIG. 11. Channel size times critical superfluid velocity as a function of temperature. The dashed line is calculated according to $v_{sc} d = (\hbar/m) [\ln(4d/a_0) - (1/4)]$.

¹⁵ R. Meservey, Phys. Rev. **127**, 995 (1962).

¹⁶ J. T. Tough, Phys. Rev. **144**, 186 (1966).

respect to the boundaries is, with good accuracy, temperature independent, as shown in Fig. 11, where we report the $v_s d$ values calculated using the hydraulic diameter as a geometrical parameter for our channel. These values are in qualitative agreement with the first threshold detected in the cylindrical channel in I, where $d = 0.9$ cm and at $T \simeq 1^\circ\text{K}$, $v_s d = 2 \times 10^{-3}$ cm²/sec. Moreover, the numerical value of $v_s d$ is in unexpected agreement with the formula for the creation of a vortex ring of a diameter equal to the hydraulic diameter; the agreement is unexpected because that formula does not include the effect of the boundaries.^{17,18} We conclude that of all the hypotheses which may be made concerning the kind of instability we are observing, the only one which is supported by our experimental results is the hypothesis that the instability is due to the creation of quantized vorticity in the superfluid. We will now discuss the hypothesis with respect to the supercritical flow characteristics which are: the anomalous velocity distribution, the anomalous temperature distribution, and the difference in the behavior of positive and negative ions. This last point is in agreement with the hypothesis, since it is known that negative ions interact with vorticity more strongly than positive ions do.¹⁹

Concerning the temperature and velocity fields, at least a qualitative agreement is reached, because if vortices are present in the superfluid, they will give rise to strong gradients in the superfluid velocity, and, as in a counterflow superfluid and normal fluid are connected through $\rho_s \mathbf{v}_s + \rho_n \mathbf{v}_n = 0$, also in the normal fluid and, of course, in the temperature. The search for quantitative agreement needs, however, the complete solution of the equation of motion including the nonlinear terms which can no longer be neglected. Also a phenomenological approach is not simple, since it requires the construction of some model for the vorticity field, capable of inducing a stationary flow pattern like the one observed. For this

purpose it might be useful to point out another possible picture of our results in the supercritical regime: In order to express the ionic beam deflection in terms of the normal fluid velocity which is the cause of the drag on the beam itself, we had to make an assumption about the shape of the streamlines. We made the reasonable assumption that the whole channel cross section is a flow tube; this is apparent in (7) where the deflection of the beam is supposed to take place along the whole lateral dimension s of the channel. If we give up that assumption, our results have to be expressed as a velocity $v_n' = v_n s'$, where s' is the lateral dimension of the flow tube (evidently $s' < s$). Then obvious considerations on the constancy of the mass flux could explain the maximum in the velocity. However, in such a case one should explain first why the flow tube is not coincident with the channel itself (the reproducibility of the results changing the walls of the channel assures that no protuberances exist on the boundaries); secondly the velocity values reported to be less than v_n^0 for some position need to be accounted for by additional assumptions such as, for instance, a dissipation of the heat energy by turbulence.

In any explanation of the supercritical flow, one should also account for the fact that the shape of the velocity distribution does not seem to depend much on the heat input up to the largest value. In particular, the distribution does not change at the crossing of the threshold detected by the trapping of negative ions, which is sometimes interpreted as due to transition to turbulence of the fluid as a whole.

A more complete determination of the velocity and temperature fields in the whole channel, together with the study of the effects on these fields of changes in the geometry of the channel and of the bath temperature in a large range, would help the understanding of the supercritical flow.

ACKNOWLEDGMENT

The authors wish to thank Professor G. Careri for discussion and advice during the course of this work.

¹⁷ J. C. Fineman and C. E. Chase, Phys. Rev. **129**, 1 (1963).

¹⁸ P. P. Craig, Phys. Letters **21**, 385 (1966).

¹⁹ G. Careri, W. D. McCormick, and F. Scaramuzzi, Phys. Letters **2**, 61 (1962).